Novel Insights into Nanopore Deformation Caused by Capillary Condensation

Gerrit Günther,[1] Johannes Prass,[2] Oskar Paris,[2] and Martin Schoen[1]

[1]*Stranski-Laboratorium für Physikalische und Theoretische Chemie, Technische Universität Berlin, Straße des 17. Juni 135, 10623 Berlin*

[2]*Abteilung Biomaterialien, Max-Planck-Institut für Kolloid- und Grenzflächenforschung, Wissenschaftspark Golm, 14424 Potsdam, Germany*

(Received 26 April 2008; published 22 August 2008)

By means of *in situ* small-angle x-ray diffraction experiments and semi-grand-canonical ensemble Monte Carlo simulations we demonstrate that sorption and condensation of a fluid confined within nanopores is capable of deforming the pore walls. At low pressures the pore is widened due to a repulsive interaction caused by collisions of the fluid molecules with the walls. At capillary condensation the pores contract abruptly on account of attractive fluid-wall interactions whereas for larger pressures they expand again. These features cannot solely be accounted for by effects related to pore-wall curvature but have to be attributed to fluid-wall dispersion forces instead.

DOI: 10.1103/PhysRevLett.101.086104 PACS numbers: 68.35.Rh, 02.70.Uu, 61.05.cf, 68.03.Fg

Fluids confined by solid substrates to spaces of nanoscopic dimension(s) exhibit properties markedly different from those of corresponding bulk fluids. These altered properties are important for many fascinating novel applications such as nanoreactors in catalysis [1], nanorheological [2], or drug delivery devices [3]. To design such devices an indispensable prerequisite is to understand how nanoconfinement affects properties of fluid matter. In this regard, understanding the unique phase behavior of confined fluids is of central importance. It becomes manifest, for example, as a narrowed gas-liquid two-phase region and a shift of the critical point relative to its location in the bulk [4–7]. However, not much attention has been paid so far to the *response* of the confining solid substrate to changes in the thermodynamic state of the fluid phase. This seems surprising in view of the fact that any substrate will "feel" the action of molecular forces. Therefore, one anticipates a deformation of pore walls during the sorption and condensation of a confined fluid phase. Such sorption strains have indeed been observed experimentally [8–10] and have been discussed in terms of both continuum elasticity [8] and phenomenological thermodynamics [9]. It is also well known that in solid-solid phase transitions elastic strains may cause a shift of the phase boundaries [11]. This poses the important question how finite stiffness of a pore wall might affect sorption and capillary condensation (CC) in nanoconfinement. In this Letter we demonstrate for the first time that sorption strains can induce an appreciable deformation of a solid substrate which in turn causes a significant shift of CC towards the bulk saturation pressure P_0. Moreover, our theoretical model is capable of reproducing semiquantitatively the measured variation of sorption strains with (bulk) pressure P.

In the experiments we employ MCM-41 silica [12] consisting of a two-dimensional hexagonal lattice of cylindrical pores (lattice parameter $a = 4.67$ nm) and use C_5H_{12} and C_5F_{12} as adsorbates. *In situ* small-angle x-ray diffraction (SAXD) measurements were conducted with synchrotron radiation at the μ-spot beam line of the BESSY II storage ring in Berlin. Details about the *in situ* sorption cell, SAXD measurements, and data treatment can be found elsewhere [13]. Figure 1 shows the diffraction profiles resulting from the pore lattice for P/P_0 below and above CC. At CC the pores fill spontaneously with a liquidlike phase. This causes the intensity of the Bragg reflections to decrease abruptly because of the reduction of the electron density difference between the silica matrix and the confined fluid. This information can be used to identify P_0^+ at CC (i.e., the bulk pressure at CC) [see Fig. 2(a)]. Besides a change in intensity the position of the Bragg reflections is also affected by changing P (see inset in Fig. 1). In Fig. 2(b) we plot the mean peak position as a function of P/P_0. A highly nonmonotonic behavior with a

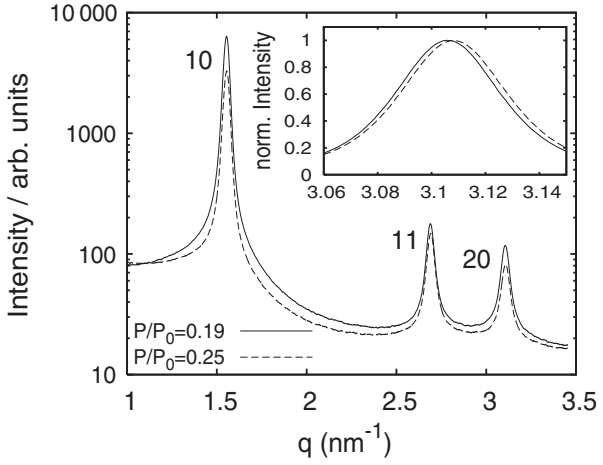

FIG. 1. X-ray diffraction pattern of C_5H_{12} in MCM-41 [$q = (4\pi/\lambda)\sin\theta$, scattering angle 2θ, wavelength $\lambda = 0.1$ nm] for two relative pressures P/P_0. Reflection indices are indicated. The inset illustrates the shift of the 20 peak at CC.

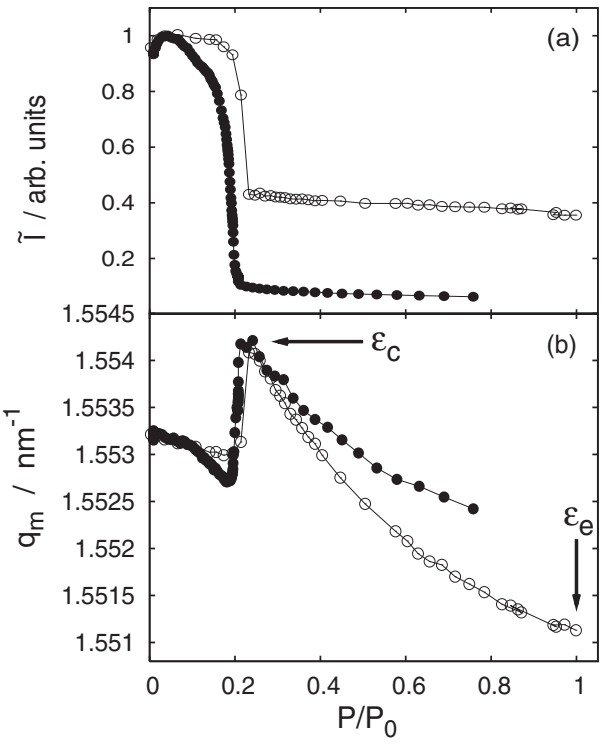

FIG. 2. Integrated intensity $\tilde{I}$ (a) and position q_m (b) of the 10 Bragg peak of C_5H_{12} (○) and C_5F_{12} (●) at $T = 17 \pm 0.1\,^{\circ}\mathrm{C}$. For a definition of ε_c and ε_e see text.

sudden increase at CC and a subsequent slow decrease is observed in these data. The independence of this effect on the "speed" of the sorption process was verified by varying the rate dP/dt (t denotes time) by a factor of 5. Because the peak shift is symmetric without appreciable change in peak width (see inset in Fig. 1) it simply reflects a change in the separation $D = 2\pi/q_m$ of the pore lattice planes. All three reflections in Fig. 1 exhibit the same qualitative and quantitative shifts suggesting a purely radial (hydrostatic) deformation of the pores. This permits us to define the homogeneous strain of the pore lattice through $\varepsilon \equiv D(P)/D(0) - 1 = q_m(0)/q_m(P) - 1$. At CC we obtain $\varepsilon_c \simeq -0.58 \times 10^{-3}$ indicating a contraction of the pore lattice which arises immediately after all pores are filled (see Fig. 2). At bulk condensation (i.e., at $P/P_0 = 1$), on the other hand, the strain $\varepsilon_e \simeq 1.35 \times 10^{-3}$ reflects a considerable expansion of the lattice now fully immersed in liquid such that $|\varepsilon_e| > 2|\varepsilon_c|$.

The characteristic features of the curves displayed in Fig. 2(b) are generic as supported by additional experiments with other classical fluids (H_2O, CH_2Br_2) and different porous media (MCM-41, SBA-15). Moreover, curves similar to the ones in Fig. 2(b) were reported for C_5H_{12} in porous silicon [9] as well as for quantum (^{4}He) and semiclassical fluids (Ne) in aerogels [10]. All of these fluids are attracted by the pore walls as reflected by $P/P_0 < 1$ which is crucial for pore contraction to occur.

In Refs. [9,10] sorption strains were rationalized on the basis of macroscopic concepts where pore curvature is a key ingredient. When the specific interfacial energy of a porous solid increases, the solid contracts to reduce its surface area. Reversly, a decrease of the interfacial energy due to fluid adsorption in nanopores leads to an expansion of the porous matrix. For cylindrical pores [8]

$$\varepsilon_e = \frac{\gamma}{R}\frac{1-2\nu}{E(1-f)} \tag{1}$$

assuming complete wetting (i.e., a vanishing contact angle) and a linear relationship between Young's modulus E and the density of MCM-41 [14]. From now on we focus exclusively on C_5H_{12} in MCM-41 as a representative example. Using a pore radius $R \simeq 1.95$ nm and a porosity $f \simeq 0.62$ both determined by nitrogen sorption, $\gamma \simeq 15 \times 10^{-3}$ J m^{-2} for the surface tension of C_5H_{12}, and $E \simeq 95$ GPa and a Poisson ratio $\nu \simeq 0.25$ of the silica matrix [14], we estimate $\varepsilon_e \simeq 0.11 \times 10^{-3}$. This value is smaller than the experimental one ($\varepsilon \simeq 1.35 \times 10^{-3}$) by roughly an order of magnitude.

The contraction of the pores at CC (see Fig. 2) has often been explained by the action of a negative hydrostatic pressure defined by the Laplace pressure $2\gamma/R^*$, where R^* is the radius of the hemispherical meniscus separating a liquidlike and a vaporlike phase [9,10,15]. The difference between ε_e and ε_c is then mainly governed by a change in sign and a different mean curvature of the film adsorbed on cylindrical pore walls ($\propto 1/R$) in the expanded and the hemispherical shape of the meniscus ($\propto 2/R^*$) in the contracted state. Because γ, ν, E, and f remain unchanged as sorption progresses, and $R^* \approx R$ at CC, one expects $\varepsilon_c \approx -2\varepsilon_e$. This is not confirmed experimentally, and the estimated value $\varepsilon_c \simeq -0.22 \times 10^{-3}$ is again considerably smaller than the experimental one. Because experimental values of ε_c and ε_e are in serious disagreement with the above estimates, we conclude that curvature effects cannot fully explain the observed variation of sorption strains in nanoscopic pores. Moreover, macroscopic concepts delineated above cannot account for the experimental variation of ε over the range $0 \leq P/P_0 \leq 1$.

If not the curvature of the pores, what other feature may be responsible for the variation of sorption strains displayed in Fig. 2(b)? In this regard it has already been noted quite some time ago by Ash *et al.* [16] that a contribution from dispersion forces may lead to repulsion or attraction between a fluid phase and its confining substrates. Balbuena *et al.* [17] showed that the associated solvation pressure exhibits a dependence on P/P_0 very similar to the variation of the strain measured in this work. Assuming deformable pore walls and Hooke's law to be valid, the data presented in Ref. [17] prompt us to conclude that dispersion forces may largely be responsible for the experimental variation of ε with P/P_0.

To test this hypothesis we perform Monte Carlo simulations in a semigrand canonical ensemble (SGCMC) in which the thermodynamic state of the system is described by its temperature T, chemical potential μ of the confined

fluid, a fixed number of substrate atoms N_s, and an elastic energy term that determines size and shape of the model system (see, for example, Chap. 6 in Ref. [7]). The fluid is composed of spherically symmetric molecules of the Lennard-Jones (LJ) type where we adjust σ to 0.3 nm to mimic fluid C_5H_{12} [18]. This fluid is confined by two substrates (slit-pore) separated by a distance $s_z = 6.8\sigma$. The substrate separation is chosen by equating the ratio of pore volume to substrate area of the model system to that characteristic of the experimental system. Thereby the "degree of confinement" in both systems is preserved irrespective of differences in pore geometry [19].

In the model each substrate is composed of atoms of the same size as the fluid molecules. These atoms are distributed such that their equilibrium positions comport with the (100) plane of the face-centered cubic lattice. On account of their thermal energy and interactions with fluid molecules, substrate atoms are able to depart from their equilibrium positions. In other words, substrate atoms "respond" to the configuration of confined fluid molecules. More specifically, the configurational energy of the model system may be cast as $U(\boldsymbol{R}, \boldsymbol{R}_s; \kappa) = U_{\mathrm{ff}}(\boldsymbol{R}) + U_{\mathrm{fs}}(\boldsymbol{R}, \boldsymbol{R}_s) + U_{\mathrm{ss}}(\boldsymbol{R}_s; \kappa)$ where the indices refer to fluid-fluid (ff), fluid-solid (fs), and solid-solid (ss) interactions, respectively. The $3N$- and $6N_s$-dimensional vectors $\boldsymbol{R}$ and $\boldsymbol{R}_s$ represent configurations of N fluid and $2N_s$ substrate atoms, respectively. Here, $U_{\mathrm{ff}}(\boldsymbol{R})$ and $U_{\mathrm{fs}}(\boldsymbol{R}, \boldsymbol{R}_s)$ are computed via pairwise additive LJ interactions; $U_{\mathrm{ss}}(\boldsymbol{R}_s; \kappa)$ consists of two contributions. One accounts for the interaction between neighboring substrate atoms. We again model these interactions via the LJ potential assuming the same potential parameters $\varepsilon_{\mathrm{LJ}}$ and σ_{LJ} as for U_{ff} and U_{fs}. The second contribution to U_{ss} arises from a harmonic potential binding substrate atoms to their equilibrium lattice sites. The binding strength is controlled by a sufficiently large "stiffness" parameter κ to prevent the substrates from melting. In the limit $\kappa \to \infty$ substrate atoms stay at their equilibrium sites such that the substrates remain undeformed and therefore $U(\boldsymbol{R}, \boldsymbol{R}_s; \kappa) \to U(\boldsymbol{R}) = U_{\mathrm{ff}}(\boldsymbol{R}) + U_{\mathrm{fs}}(\boldsymbol{R})$. In this limiting case the confining substrates can be treated as a static external field imposed on the fluid molecules as it is done in the overwhelming number of theoretical studies of nanoconfined fluids to date [7]. However, in the more general case where U depends on both $\boldsymbol{R}$ and $\boldsymbol{R}_s$ the theoretical treatment is more complicated. This is because then the configuration integral involves an integration of the Boltzmann factor $\exp[-\beta U(\boldsymbol{R}, \boldsymbol{R}_s; \kappa)]$ over configurations of both fluid molecules and substrate atoms [18,20]. In other words, for finite κ the substrates cannot be treated as an external field so that the SGCMC simulations are quite computationally demanding.

The SGCMC simulations proceed in a standard manner [7]. However, because N_s is fixed creation and destruction are not attempted for substrate atoms. Using concepts of thermodynamic perturbation theory explained elsewhere [18] we have access to the *bulk* pressure P_0^+ at CC. Note that P_0^+ will generally differ between experimental and model systems because of various assumptions made for the model system. Another key quantity is the *effective* pore width $s_z^{\mathrm{eff}}(\kappa)$ where

$$\lim_{\kappa\to\infty} s_z^{\mathrm{eff}}(\kappa) \equiv \frac{1}{N_s} \lim_{\kappa\to\infty} \left\langle \sum_{i=1}^{N_s} |z_i^{[2]} - z_i^{[1]}| \right\rangle_\kappa = s_z \qquad (2)$$

and $z_i^{[k]}$ is the z coordinate of atom i in substrate k. Angular brackets indicate an average over configurations in the semigrand canonical ensemble. With the aid of Eq. (2) we define the strain $\xi \equiv s_z^{\mathrm{eff}}(\kappa)/s_z - 1$ as a quantitative integral measure of pore deformation which can be compared with the experimentally measured lattice strain ε. Figure 3 shows that for $P/P_0^+ > 0$ the effective pore width increases slightly initially. At CC (i.e., at $P/P_0^+ \simeq 1$) the pore abruptly shrinks and then expands again as P increases further. It is remarkable that both experimental and theoretical data plotted together in Fig. 3 agree very well qualitatively and even quantitatively for a certain range of pressures despite the smallness of the strain. The agreement is particularly gratifying because the theoretical model is rather crude in that it assumes the LJ potential with the same set of potential parameters $\{\varepsilon_{\mathrm{LJ}}, \sigma_{\mathrm{LJ}}\}$ for all intermolecular interactions, perceives C_5H_{12} molecules as spheres, and uses a single slit—rather than an ordered array of cylindrical pores.

How does pore deformation affect CC? To address this question we compute the grand-potential density ω of the confined fluid as we explain in detail in Ref. [18]. In general, $(\partial\omega/\partial\mu)_{\{\cdot\}} = -\rho$ where ρ is the mean density of the fluid phase and $\{\cdot\}$ is shorthand notation to indicate that all other thermodynamic variables are held constant. Along any subcritical isotherm ω is a continuous function of P (or μ) [7]. However, its slope will change discontinuously at P_0^+ at which phases of different (mean) density (e.g., confined gaslike and liquidlike phases) coexist. As

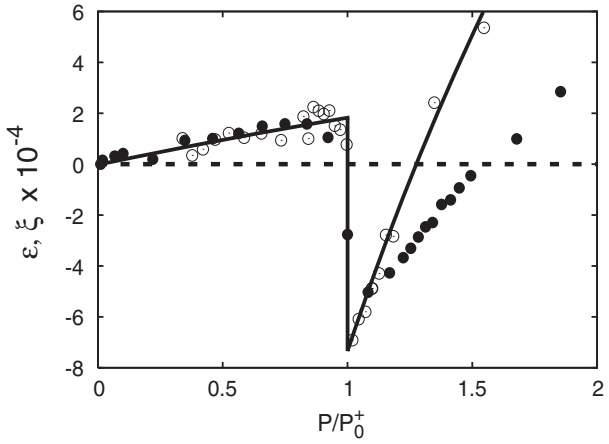

FIG. 3. Sorption strains trains ε for C_5H_{12} as a functions of P/P_0^+; (experiment) (●), ξ (theory) (○) ($\kappa\sigma_{\mathrm{LJ}}^2/\varepsilon_{\mathrm{LJ}} = 30$). The full line is intended to guide the eye. In the limit $\kappa \to \infty$ (rigid substrate), $\xi = 0$ (dashed line).

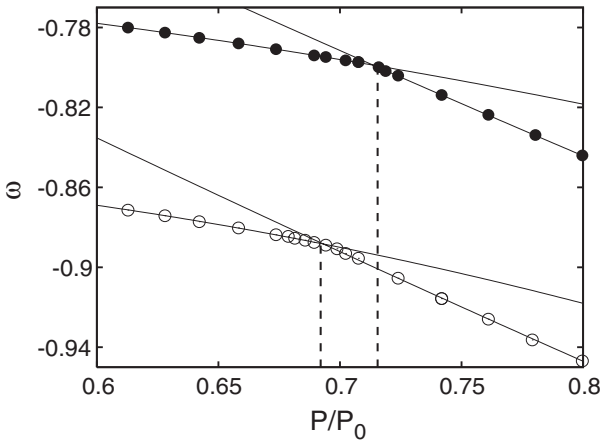

FIG. 4. Grand-potential density ω as a function of reduced pressure P/P_0 ($k_BT/\varepsilon_{LJ} = 1.0$). Vertical dashed lines demarcate the pressure P_0^+ at CC; $\kappa\sigma_{LJ}^2/\varepsilon_{LJ} = 10^4$ (○) (quasirigid substrate) and $\kappa\sigma_{LJ}^2/\varepsilon_{LJ} = 30$ (●).

anticipated, Fig. 4 reveals a discontinuous change of the slope of ω at CC. Branches of ω for $P < P_0^+$ and $P > P_0^+$ refer to gaslike and liquidlike phases, respectively. However, P_0^+ depends on the deformation of the substrate. The shift of P_0^+ relative to the value for rigid substrates can be rationalized as follows. In the limit $\kappa = 0$ substrate atoms are no longer bound to their equilibrium lattice sites but are free to move. The original confined fluid therefore becomes equivalent to the bulk. In fact, ''substrate'' atoms and fluid molecules become indistinguishable on account of our choice of the same LJ potential parameters for all intermolecular interactions. One therefore anticipates $P_0^+/P_0 = 1$ if $\kappa = 0$. For finite κ, on the other hand, the confined fluid should therefore exhibit a phase transition somewhere in between the value of P_0^+ characteristic of the rigid substrate and $P_0^+/P_0 = 1$ as shown in Fig. 4. Finally, we stress that results for the model system plotted in Figs. 3 and 4 are qualitatively independent of T and s_z [18]. Thus, both the variation of ξ (ε) with P and that of P_0^+ with κ are *generic* features associated with sorption strains.

We conclude that using a simple model system in SGCMC, the strain behavior measured for C_5H_{12} in MCM-41 can be quite well reproduced over a wide range of thermodynamic states. In particular, our simulations reveal a continuous expansion of the pore with increasing P intermitted by a sudden contraction upon CC, in nearly perfect agreement with the experiment, even though the geometries are markedly different (slit pores vs cylindrical pores). This suggests that dispersion forces make a dominant contribution to the sorption strains, while curvature effects are less important. In addition, pore deformation causes a shift of the phase transition towards that in the bulk. Compared with the ideal case of rigid pore walls the shift is of the order of a few per cent and should thus be observable experimentally *in principle*. However, to change the stiffness of an experimental system while keeping all other parameters fixed is challenging and could not be realized here.

Nevertheless, the present study demonstrates a synergistic effect, that is the substrate responds to the thermodynamic state of the confined fluid which in turn affects the fluid's phase behavior. This synergistic effect is also expected to affect other types of phase transitions in nanoconfinement. For example, undercooled nanoconfined water does not freeze in the immediate vicinity of but only at larger distances from the pore walls, presumably on account of severe strains that prevent such vicinal water from forming solidlike structures [21]. These strains should be capable of deforming the pore walls similar to what is observed here. Another example are nanoconfined mesophases of anisometric molecules where molecular packing and orientation should exert strains on the pore walls. Implications from sorption strains on the phase behavior and vice versa might be expected particularly for fluids in very compliant nanoporous systems. A case of special interest in this respect is the action of water in biological tissues, e.g., the movements of plants driven by changes in humidity [22].

We acknowledge financial support from DFG (No. SFB 448) and thank G. H. Findenegg, S. Jähnert, C. Li, S. Siegel, and S. H. L. Klapp for support and discussions.

[1] S. A. Soper *et al.*, J. Chromatogr. A **853**, 107 (1999).
[2] B. Cross and J. Crassou, Eur. Phys. J. E **14**, 249 (2004).
[3] X. R. Teng *et al.*, Langmuir **24**, 383 (2008).
[4] R. Evans and A. O. Parry, J. Phys. Condens. Matter **2**, SA15 (1990).
[5] L. D. Gelb *et al.*, Rep. Prog. Phys. **62**, 1573 (1999).
[6] K. Binder *et al.*, Comput. Phys. Commun. **177**, 140 (2007).
[7] M. Schoen and S. H. L. Klapp, *Reviews in Computational Chemistry*, edited by K. B. Lipkowitz *et al.* (Wiley-VCH, Hoboken, 2007), Vol. 24.
[8] G. W. Scherer, J. Am. Ceram. Soc. **69**, 473 (1986).
[9] G. Dolino *et al.*, Phys. Rev. B **54**, 17919 (1996).
[10] T. Herman *et al.*, Phys. Rev. B **73**, 094127 (2006).
[11] K. Binder and P. Fratzl, in *Materials Science and Technology*, edited by G. Kostorz (Wiley-VCH, Weinheim, 2001), Vol. 5, pp. 409–480.
[12] C. T. Kresge *et al.*, Nature (London) **359**, 710 (1992).
[13] G. Zickler *et al.*, Phys. Rev. B **73**, 184109 (2006).
[14] H. Fan *et al.*, Nature Mater. **6**, 418 (2007).
[15] C. Schaefer *et al.*, Phys. Rev. Lett. **100**, 175701 (2008).
[16] S. G. Ash *et al.*, J. Chem. Soc., Faraday Trans. 2 **69**, 1256 (1973).
[17] P. B. Balbuena *et al.*, J. Phys. Chem. **97**, 937 (1993).
[18] G. Günther and M. Schoen, Mol. Simul. (to be published).
[19] G. Rother *et al.*, J. Chem. Phys. **120**, 11864 (2004).
[20] D. J. Diestler and M. Schoen, J. Chem. Phys. **104**, 6784 (1996).
[21] A. Schreiber *et al.*, Phys. Chem. Chem. Phys. **3**, 1185 (2001).
[22] R. Elbaum *et al.*, Science **316**, 884 (2007).